

# Traces of Carnian volcanic activity in the Transdanubian Range, Hungary

István Dunkl<sup>1</sup>, Éva Farics<sup>2</sup>, Sándor Józsa<sup>3</sup>, Réka Lukács<sup>4</sup>, János Haas<sup>5</sup>, Tamás Budai<sup>2</sup>

<sup>1</sup> University of Göttingen, Geoscience Center, Department of Sedimentology and Environmental Geology, Göttingen, Germany

<sup>2</sup> University of Pécs, Department of Geology and Meteorology, Pécs, Hungary

<sup>3</sup> Eötvös Loránd University, Department of Petrology and Geochemistry, Budapest, Hungary

<sup>4</sup> MTA-ELTE Volcanology Research Group, Budapest, Hungary

<sup>5</sup> MTA-ELTE Geological, Geophysical and Space Science Research Group, Budapest, Hungary

corresponding author: Éva Farics, [eva.gyorfy@gmail.com](mailto:eva.gyorfy@gmail.com), +36-306590625

## Acknowledgements

The CL images of the dated zircons were prepared by the kind help of Andreas Kronz (Göttingen). Guido Meinhold (Keele University) sharpened the English text of the manuscript. Discussions with Franz Neubauer (Salzburg), the suggestions of Vincenzo Picotti, Christoph Breitkreuz, an unknown reviewer and the editorial handling of Wolf-Christian Dullo significantly improved the quality of the manuscript. Many thanks for their kind help. The project has been supported by the European Union, co-financed by the European Social Fund (EFOP-3.6.1.-16-2016-00004).

## Abstract

The South Alpine–Dinaridic realm was affected by igneous activity in the Middle Triassic; the marine carbonate platforms and the adjacent basins contain highly variable intrusive-

26 volcanic assemblages. We studied the petrography and determined the zircon U–Pb ages of  
27 the Triassic volcanic products in the Transdanubian Range. The geochemical features and  
28 thus the geodynamic context of the magmatism is badly known, as the rocks experienced  
29 variable chemical alteration. The exact duration of the igneous activity is also poorly  
30 constrained, as the geochronological data of the former studies were obtained mostly by the  
31 weathering-sensitive K–Ar and Rb–Sr methods and thus some data even being younger than  
32 the age of the stratigraphic cover. The presence of andesite dikes and of pebbles and cobbles  
33 (< 20cm) of basalt, andesite, rhyolite and of rhyolitic tuff in the Triassic carbonate platform  
34 deposits indicate that within the Transdanubian Range formed a volcanic complex in Triassic.  
35 The major mineralogical and geochemical features of the Transdanubian igneous suite is  
36 similar to the Triassic formations in the Southern Alps. However, dissimilar zircon  
37 composition excludes the immediate relationship of the zircon-bearing silicic formations in  
38 the two tectonic units. New U–Pb ages show that the beginning of the volcanic activity is  
39 probably coeval with the eruption of the widespread "pietra verde" trachytic tuffs in the Upper  
40 Anisian–Ladinian successions, but the majority of the ages is younger than those ash layers.  
41 The new age constraints give a bench-mark for the termination of the volcanic activity in  
42 Carnian time in the Transdanubian Range.

43

#### 44 **Keywords**

45 Triassic, volcanism, U–Pb geochronology, Transdanubian Range, Southern Alps

## 46 **Introduction**

47 The Transdanubian Range Unit is a part of the Alcapa Mega-unit (Haas 2013). This fault-  
48 bordered terrane – including the Bakony Mountains and Buda Hills – was located close to the  
49 Southern Alps at the northwesternmost edge of the opening Vardar ocean during the Middle-  
50 Late Triassic and it belonged to the wide carbonate shelf of the western Tethys (e.g. Kázmér  
51 and Kovács 1985, Haas et al. 1995, Vörös 2000). Presence of volcanic tuffs in the Triassic  
52 succession of the Transdanubian Range had been recognised already by Böckh (1873) in the  
53 Bakony Mountains (Fig. 1). According to Lóczy (1916), the Ladinian "Buchenstein beds" are  
54 made up of siliceous limestones, marls and "pietra verde" tuffs. These pyroclastic layers have  
55 trachytic composition and they consist of mainly sanidine, biotite, few quartz and secondary  
56 minerals (Szabó and Ravasz 1970; Ravasz 1973). Literature data and the present study  
57 provide evidence that, in addition to the late Anisian–Ladinian "pietra verde" pyroclastic fall  
58 deposits present in the Southern Alps and derived from an unknown, remote volcanic centre, a  
59 Middle to Late Triassic volcanism also occurred within or close to the Transdanubian Range.  
60 This volcanic activity was documented by Raincsák (1980) and Budai et al. (2001) in the  
61 Middle Triassic succession of the Bakony Mountains. A comparison of the Middle Triassic  
62 volcanic successions of the Bakony Mountains, Bükk Mountains, Southern Alps and Northern  
63 Calcareous Alps was presented by Bechstädt and Mostler (1976), Cros and Szabó (1984),  
64 Szoldán (1990) and Harangi et al. (1996). They concluded that the Transdanubian Range may  
65 have been relatively close to the South Alpine volcanic centres, whereas the area of the  
66 Northern Calcareous Alps was located in a more distal position.  
67 This igneous activity – similarly to those of the Southern Alps – is slightly enigmatic, as it is  
68 localized in a passive margin settings during the development of carbonate platform  
69 successions. The geodynamic evaluations based on the geochemical character of the Southern  
70 Alpine and Dinaridic occurrences yielded ambiguous results, showing signs for both,

71 continental rift and magmatic arc settings (e.g. Bébien et al. 1978; Beltrán-Triviño et al.  
72 2016). Harangi et al. (1996) linked the Middle to Late Triassic volcanism to early extensional  
73 events that were followed by a more developed rifting phase in the Bükk Mountains, Bakony  
74 Mountains and Buda Hills.

75 The aim of this paper is to complete the information about the puzzle of the dissected parts of  
76 the former carbonate platform by new petrographical and geochemical data from the Triassic  
77 volcanogenic formations of the Bakony Mountains and Buda Hills and to supply new time  
78 constraints by U–Pb ages for the duration of the volcanic activity.

79

### 80 **Geological setting and traces of Triassic volcanism in the Transdanubian Range**

81 The Transdanubian Range is the uppermost unit of the Austroalpine Nappe System forming a  
82 syncline structure (e.g. Tari et al. 1992). The development of its Upper Permian to Lower  
83 Cretaceous formations shows close affinity with that of the Southern Alps (Lóczy 1916; Haas  
84 and Budai 1995). The thickest part of the sequence is made up of Triassic shallow marine  
85 carbonates (Haas 2013). The Triassic magmatic dikes, volcanic pebbles and cobbles occur in  
86 three formations in the Bakony Mountains and in the vicinity of the Buda Hills (Fig. 2).

87 (i) The Upper Anisian Vászoly Formation contains distal, several cm to max 2 dm thick,  
88 bentonitised trachytic, sometimes graded, primary fallout tuff layers (Budai et al. 1999, 2001,  
89 2015). These strata are equivalent to the slightly thicker "pietra verde" layers in the Dolomites  
90 (Mojsisovics, 1879), and they are widespread in the entire Southern Alpine–Dinaridic realm  
91 (e.g. Obenholzner 1991; Jelaska et al. 2003). The biostratigraphic assignment of these ash  
92 layers is well constrained by ammonoid, conodont and radiolarian data to be in the Reitzi  
93 Zone (Vörös 1993; Dosztály 1993; Kovács 1994; Pálfy et al. 2003). The zircon content of the  
94 ash and bentonite layers of mostly trachytic chemical character allowed highly precise U–Pb  
95 geochronology (see details below). According to the accurate biostratigraphic, isotope

96 geochronologic and paleomagnetic constraints (Márton et al. 1997) the Felsőörs section was  
97 even proposed as a candidate for a Global Stratotype Section and Point for the base of the  
98 Ladinian stage (Vörös et al. 1996, 2003).

99 (ii) Andesite dikes are known in the quarry of Szár Hill at Polgárdi and they have been  
100 detected by the Budaörs-1 and Budafok-1 cored deep drillings of the Buda Hills (Kubovics  
101 1985; Dunkl et al. 2003; Haas et al. 2017). The well exposed, gray porphyritic dikes in the  
102 Szár Hill quarry, are 5 to 10 m thick, while the apparent thicknesses of the partly fault-  
103 bounded dikes in the boreholes are between 60 to 186 m (Budaörs-1 and Budafok-1,  
104 respectively).

105 (iii) Pebbles of volcanic rocks were recognized in the Middle Triassic sequence of the Bakony  
106 Mountains (Rainsák 1980). This volcanoclastic sandstone (Inota Fm.) was correlated with  
107 the Wengen Group of the Southern Alps (Mojsisovics, 1879; Budai and Vörös 1993; Budai et  
108 al. 2001). Clasts of volcanic rocks were also found at the base of the Upper Eocene  
109 transgressive sequences of the Buda Hills (Wein 1977; Horváth and Tari 1987; Farics et al.  
110 2015). As will be discussed below, the "pietra verde" tuff originated from remote sources,  
111 while the (ii) and (iii) type formations are local volcanic products within the Transdanubian  
112 Range (Budai et al. 2001).

113 With the exception of a single U–Pb age (Haas et al. 2017), only whole-rock, biotite and  
114 hornblende K–Ar data are available from the dikes and pebbles (Balogh et al. 1983; Horváth  
115 and Tari 1987). The dated aliquots contain highly variable amounts of potassium and  
116 radiogenic argon, and they yielded a wide age range from 240 to 25 Ma. The isotopic systems  
117 have been strongly influenced either by the interaction of the dikes with the carbonate host  
118 rocks or by the weathering of the pebbles. Thus, their significance for the timing of eruptions  
119 and on the duration of the volcanic activity is weak.

120

121 **Triassic igneous activity in the South Alpine realm and their geochronological**  
122 **constraints**

123 According to the palaeogeographic reconstructions, the Transdanubian Range was located in  
124 the neighbourhood of the Southern Alps before the Alpine orogeny (Kázmér and Kovács  
125 1985; Haas et al. 1995; Schmid et al. 2008). Thus, it is necessary to insert a short review of  
126 the well exposed and studied Triassic igneous formations of the Southern Alps before the  
127 evaluation of our new results from the Transdanubian Range.

128 The "pietra verde" tuff layers (e.g. Obenholzner 1991) were dated both in the Alps and in the  
129 Bakony Mountains by high precision and accuracy and those data were contributed even to  
130 the global calibration of the Triassic chronostratigraphic scale (Mundil et al. 1996, 2010;  
131 Pálfy et al. 2003; Brack et al. 2005; Furrer et al. 2008; Stockar et al. 2012; Wotzlaw et al.  
132 2018). The ID-TIMS data reveal that these trachytic eruptions took place between 242 and  
133 237 Ma.

134 The Predazzo Complex is the largest of the Triassic intrusive igneous bodies of the Eastern  
135 Southern Alps. The intrusive rocks show wide variation in composition: monzonite is the  
136 dominant rock type, but monzodiorite, monzogabbro, gabbro with pyroxenite, granite, quartz-  
137 syenite and syenite, also occur (Lucchini et al. 1982; Menegazzo et al. 1995; Visonà 1997;  
138 Carraro and Visonà 2003; Casetta et al. 2018). The dike rocks are also highly diverse:  
139 latibasalt, latiandesite, K-basanite, monzosyenite, aplite and lamprophyre were reported by  
140 Gallitelli and Simboli (1971). Some of the carbonate platforms of the Dolomites are covered  
141 by subaerial basaltic flows (e.g. Monte Agnello), but submarine formations like pillow lavas  
142 and hyaloclastite-rich volcano-sedimentary formations are more common in the intra-platform  
143 basin fill (Gaetani et al. 1981; Preto et al. 2001; Bosellini et al. 2003; Budai et al. 2005;  
144 Németh and Budai 2009). In the western Southern Alps the Montecampione subvolcanic

145 complex shows slightly more alkaline character, but the sodium, potassium and trace element  
146 contents were probably influenced by intense fluid circulation (Armienti et al. 2003).  
147 The geodynamic interpretation of this magmatism is debated because beyond the obvious  
148 traces of Triassic syn-sedimentary extensional tectonics manifested e.g. by half-grabens  
149 (Bertotti et al. 1993; Budai and Vörös 1993, 2006; Velledits 2006), strike-slip and  
150 compressional tectonics make the image more complex (Castellarin and Rossi 1981;  
151 Blendinger 1984; Castellarin et al. 1988). However, the wide spectrum of rock types and their  
152 trace elements and Hf-isotope systematics would fit to an extensional regime. Beltrán-Triviño  
153 et al. (2016) related the Triassic magmatism to an asymmetrical continental rifting process  
154 that affected the entire Southern Alps and the adjacent areas. The geodynamic evaluation of  
155 the Triassic volcanism in the Dinarides resulted in similar dilemma; the compositional  
156 spectrum of the lithologies (from basalt to rhyolite) and their geochemical features match  
157 neither to the rifting nor to the arc settings (Bébién et al. 1978).  
158 Evaluating the age constraints from the Predazzo Complex and from other Triassic volcanic  
159 formations we should distinguish between weathering/alteration-sensitive and more robust  
160 geochronometers. The Rb–Sr and K–Ar ages scatter between 230 and 204 Ma (Borsi and  
161 Ferrara 1967; Borsi et al. 1968; Ferrara and Innocenti 1974; Webb 1982; Crisci et al. 1984;  
162 Laurenzi et al. 1994; Visonà 1997; Balogh and Németh 2005). Similarly to the Bakony  
163 Mountains, some of these ages clearly post-date the stratigraphically proven age range of the  
164 volcanic activity. U–Pb and Sm–Nd ages (246 to 224 Ma) are available only from a few  
165 igneous bodies of the Southern Alps (Zanetti et al. 2013; Storck et al. 2018), Eisenkappel  
166 pluton (Lippolt et al. 1974; Miller et al. 2011), Western Carpathians (Putiš et al. 2000), Bükk  
167 Mountains (Haas et al. 2011; Kövér et al, 2018), Eastern Alps, and northwestern Dinarides  
168 (Neubauer et al. 2014).  
169

170 **Samples**

171 We collected "pietra verde" tuff, volcanogenic sandstone and conglomerate drilling core and  
172 outcrop samples from Triassic strata and from the base of the Eocene transgressive sequence  
173 that unconformably covers the partly eroded Triassic successions. Actually, all known and  
174 accessible volcanic formations (Vászoly Fm., Inota Fm.) were sampled in the Bakony  
175 Mountains and Buda Hills. Additionally, we have taken seven pilot samples for  
176 geochronology and zircon geochemistry from the Triassic igneous formations of the eastern  
177 Southern Alps. The localities of the dated samples are listed in Table 1, and a list of  
178 petrographically analysed samples is given in the Electronic Supplementary Material  
179 (ESM\_1.xls). In order to represent properly the sources of the coarse volcanic fragments we  
180 performed pebble population dating (PPD-method; Dunkl et al. 2009) on selected and  
181 amalgamated andesite, and acid volcanite + ignimbrite pebbles. These "PPD" samples were  
182 composed of a representative selection of 16 to 54 equal-sized volcanic rock pebbles or  
183 pebble fragments.

184

185 **Analytical method**

186 For the petrographic investigation of the volcanic rocks Olympus BH2 polarization  
187 microscope was used. The composition of feldspar, pyroxene, amphibole was determined  
188 with AMRAY 1830 scanning electron microscope with EDAX PV 9800 ED spectrometer at  
189 the Eötvös University, Budapest. Major, trace and rare earth elements of the whole rock  
190 samples were measured at the University of Göttingen by X-ray fluorescence analysis, and by  
191 ICP-AES & ICP-MS techniques in ACME Labs (Vancouver).  
192 Zircon crystals were fixed on a double-side adhesive tape stuck on a thick glass plate and  
193 embedded in a 25 mm diameter epoxy mount. The crystal mounts were lapped by 2500 mesh  
194 SiC paper and polished by 9, 3 and 1 micron diamond suspensions. Cathodoluminescence



195 images were obtained using a JEOL JXA 8900 electron microprobe at the University of  
196 Göttingen in order to study the internal structure of the zircon crystals and to select  
197 homogeneous parts for in-situ age determination.

198 The U-Pb dating was performed by laser-ablation single-collector sector-field inductively  
199 coupled plasma mass spectrometry (LA-SF-ICP-MS). The method employed for our analyses  
200 has been described in details by Frei and Gerdes (2009). We used a Thermo Element 2 mass  
201 spectrometer coupled to a Resonetics excimer laser with Laurin Technic 155 constant  
202 geometry ablation cell. All age data presented here were obtained by single spot analyses with  
203 a laser beam diameter of 33  $\mu\text{m}$  and a crater depth of approximately 10  $\mu\text{m}$ . The laser was  
204 fired at a repetition rate of 5 Hz and at nominal laser energy output of 25 %. The data  
205 reduction is based on the processing of ca. 50 selected time slices (corresponding ca. 14  
206 seconds) starting ca. 3 sec. after the beginning of the signal. If the ablation hit zones or  
207 inclusions with highly variable actinide concentrations or isotope ratios then the integration  
208 interval was slightly resized or the analysis was discarded (~1% of the spots). The individual  
209 time slices were tested for possible outliers by an iterative Grubbs test (applied at P=5%  
210 level). The age calculation and quality control are based on standard-sample bracketing using  
211 GJ-1 zircon reference material (Jackson et al. 2004). For further control the Plešovice zircon  
212 (Sláma et al. 2008), the 91500 zircon (Wiedenbeck et al. 1995) and the FC-1 zircon (Paces  
213 and Miller 1993) were analysed as "secondary standards". The results obtained on the zircon  
214 reference materials express the precision and the accuracy of the dating method applied (see  
215 details in Electronic Supplementary Material ESM\_2.pdf). Drift- and fractionation corrections  
216 and data reductions were performed by our in-house software (UranOS; Dunkl et al. 2008).  
217 The concordia plots were constructed by the help of Isoplot/Ex 3.0 (Ludwig 2012).  
218

219 **Results**

220 *Petrography of the Triassic volcanic products of the Transdanubian Range*

221

222 *Dike rocks*

223 The Triassic volcanic formations are often altered, most of the phenocrysts are replaced by  
224 secondary minerals and we can observe only pseudomorphs after them. Due to strong  
225 alteration, it is often not possible to achieve a reliable geochemical classification. In these  
226 cases, we characterized the samples according to their petrographic features.

227 The lava and dike rocks are mostly comprised of andesite. The unaltered porphyritic andesite  
228 contains large zoned labradorite-andesine and small andesine-basic oligoclase crystals,  
229 hypersthene orthopyroxene, and subordinately augitic clinopyroxene and biotite. The  
230 amphibole is hornblende in composition and it was found only in the andesite dikes of the  
231 Szár Hill (Fig. 3a). Ilmenite, apatite, garnet, magnetite, zircon and monazite are the accessory  
232 minerals. The phenocrysts are often replaced by clay and opaque minerals, chlorite,  
233 chalcedony, carbonate, and sericite (Figs. 3b and 3c). In the fine-grained groundmass thin  
234 laths of plagioclase, and variable amounts of partly altered (chloritized) glass are present. In  
235 the samples from the lower part of the dike in Budaörs-1 well intense K-metasomatism was  
236 detected, the plagioclase altered to K-feldspar (Fig. 3d). Complete alteration of the  
237 groundmass to secondary silica is observed, especially in the volcanic clasts of the Eocene  
238 conglomerates. The vesicles are filled mostly by chalcedony and glauconite. The andesite  
239 often contains microdiorite inclusions.

240

241 *Triassic volcanogenic sandstones and conglomerates*

242 In the Bakony Mountains and in the Strázsa Hill quarry (Zsámbék), the volcanogenic  
243 sandstones and conglomerates form clast-supported, polymict deposits. Subangular to

244 subrounded mafic–intermediate volcanic clasts are usually much larger (up to 20 cm) and  
245 more common than the subrounded acidic volcanic clasts ( $\leq 3$  cm). The phenocrysts are  
246 completely altered to secondary minerals, but three types of mafic lithologies can be  
247 distinguished. One type contains abundant vesicles and a few pseudomorphs after plagioclase,  
248 pyroxene and olivine phenocrysts (Fig. 3e). The other type has an intersertal texture with  
249 plagioclase microliths in the groundmass and few pseudomorphs after plagioclase and mafic  
250 phenocrysts. The third type is microgabbro with intergranular texture; the xenomorphic mafic  
251 minerals occur in the spaces among the plagioclase laths. Some of the andesites are  
252 characterized by the presence of porphyric labradorite-andesine plagioclase, hypersthene  
253 orthopyroxene and few biotite as well as laths of andesine-basic oligoclase plagioclase in the  
254 groundmass (Figs. 3f and 3g). In several pebbles the plagioclase has been replaced by K-  
255 feldspar due to intense K-metasomatism. The latite-trachyte pebbles are characteristically  
256 different from the andesite, they contain primary alkali feldspar (K-feldspar) and less  
257 plagioclase. Another type of basaltic/andesitic clasts is vesicle-rich and contains only  
258 plagioclase phenocrysts (Fig. 3g). The acidic volcanic pebbles consist of quartz, K-feldspar  
259 and biotite. Rhyolite contains dark and light flow banding and has poorly developed  
260 micropoikilitic texture (Fig. 3h). Three types of devitrificated rhyolite lava and rhyolite tuff  
261 can be found. The first one consists of mostly pumice and few glass shards with very few  
262 labradorite phenocrysts and more acidic plagioclase microliths. The second one has perlitic  
263 texture, and the third one has spherulitic texture. Acidic tuff clasts (only in the Strázsa Hill  
264 quarry) contain pumice and Y-shaped glass shards, pseudomorphs after K-feldspar and biotite  
265 flakes, as well as lithic fragments (Fig. 3i). Besides the lithoclasts, the labradorite-basic  
266 oligoclase, hypersthene orthopyroxene, hornblende amphibole, biotite, augitic clinopyroxene  
267 and altered olivine crystal fragments are in the volcanogenic sandstone layers of the Bakony

268 Mountains, as well as strongly altered plagioclase (mostly altered to K-feldspar), biotite,  
269 pyroxene, quartz in the volcanogenic sandstones of the Strázsa Hill quarry.

270

### 271 *Volcanic clasts from the base of Eocene conglomerates*

272 In the basal layers of the Eocene conglomerate of the Buda Hills we found mostly andesite  
273 and acidic lava and tuff pebbles (Fig. 3j).

274

### 275 **Geochemistry**

276

277 The volcanic rocks showing mafic petrographical characters are strongly altered and are not  
278 suitable for geochemical analysis (LOI up to 20%; Electronic Supplementary Material  
279 ESM\_3.xls). However, there are some less altered intermediate and felsic volcanic samples  
280 from Buda Hills, Strázsa Hill quarry and Bakony Mountains that yielded useful major and  
281 trace element data. Nevertheless, these rocks still have some significant LOI content,  
282 therefore their compositions should be evaluated with caution. All samples are plotted on the  
283 total alkali versus silica (TAS) diagram after recalculation to anhydrous basis (Fig. 4). They  
284 fall mostly into the andesite field, whereas a few samples are rhyolite. The samples showing  
285 trachyandesite to trachyte compositions could have experienced some alkali enrichment  
286 during alteration, whereas alkali leaching can not be excluded in case of a few samples.  
287 Immobility trace elements can be effectively used as indicators for rock types (Pearce 1996)  
288 even for altered and slightly metamorphosed rocks. Based on the Nb/Y vs. Zr/TiO<sub>2</sub> diagram  
289 the analysed rocks are mainly andesite in spite of their TAS classification.

290 The immobile trace elements suggest subalkaline affinity (Fig. 4), and they plot in the active  
291 continental margins field in the tectonomagmatic setting discrimination diagram of Gorton  
292 and Schandl (2000) for felsic and intermediate rocks (Fig. 5). The samples having andesitic

293 petrographical character usually show enrichment in LIL elements (Ba, Rb, Th, U) and  
294 negative anomalies for certain HFS elements (Nb, P, Ti), although the latter ones are not  
295 always pronounced (Fig. 6). The REE patterns of most andesite samples are similar with  
296 negative Eu anomaly, suggesting plagioclase fractionation. Notably the samples classified as  
297 rhyolite and trachyte based on their petrographic character show much larger compositional  
298 distribution, having lower and higher values for LREE. This compositional variation can be  
299 traced also on the multivariate trace element diagrams (Fig. 6).

300

### 301 *Mineral chemistry*

302

303 The strongly altered character of the studied volcanic rocks is reflected in their mineral  
304 assemblage, since only a few samples contain detectable mafic minerals, such as pyroxene  
305 and amphibole. Pyroxene is present only in a few mafic and intermediate volcanic samples of  
306 the Transdanubian Range. The orthopyroxene has a composition from En<sub>57</sub> to 53 mol%,  
307 while clinopyroxene is of augitic composition. Amphibole can be found only in the samples  
308 from Szár Hill quarry and wells of Bakony Mountains, they are Mg-hornblende and  
309 tschermakite. Plagioclase shows a wide compositional range with An content ranging from 10  
310 to 70 mol% (ESM\_4.xls and ESM\_5.pdf).

311

### 312 *Zircon U–Pb Geochronology*

313

314 Laser-ablation ICPMS U–Pb geochronology was performed on 485 separated, CL-mapped  
315 zircon crystals in the GÖochron Laboratories of the University of Göttingen. Some samples  
316 have poor zircon yield, due to either their mafic character, or due to the small amount of the  
317 available drilling cores. Ca. 20% of the obtained ages were much older or younger than  
318 Triassic; these spots were measured probably on xenocrystals of the Triassic magmatites or on

319 Cenozoic igneous pebbles that were mixed into the PPD samples pooled from the Eocene  
320 strata. A synopsis of the results is listed in Table 2, the detailed analytical data are given in the  
321 Electronic Supplementary Material (ESM\_6.xls and ESM\_7.pdf). Where possible, the ages  
322 were calculated as concordia age, otherwise we considered only those analyses that are  $100 \pm$   
323  $10\%$  concordant and applied the Isoplot "ZircAge" algorithm in order to express a mean age  
324 for the crystallization of the most reliable zircon population according to Ludwig (2012). The  
325 age data are grouped according to major types of the samples and the mean values with the  
326 uncertainty intervals are plotted in Fig. 7.

327 Before the presentation of the results from Transdanubian Range we should consider the U–  
328 Pb data obtained on the Eisenkappel intrusion. This narrow granitoid body is situated along  
329 the Periadriatic Line and was dated already by several methods and yielded  $227 \pm 7$  Ma  
330 biotite and  $244 \pm 8$  Ma hornblende K–Ar ages,  $230 \pm 5$  Ma titanite U–Pb age and  $238.4 \pm 1.9$   
331 Ma and  $242.1 \pm 2.1$  Ma garnet-whole rock Sm–Nd ages (Lippolt et al. 1974; Miller et al.  
332 2011). Our new laser ablation zircon U–Pb ages ( $234.1 \pm 2.5$  and  $231.2 +5.8 -2.2$  Ma) are  
333 close to the formerly measured titanite U–Pb ages and obviously younger than the Sm–Nd  
334 data.

335 Component analysis was performed on the  $\pm 10\%$  concordant single-crystal  $^{206}\text{Pb}/^{238}\text{U}$  ages  
336 determined in the volcanoclastic formations. The individual samples contain relatively low  
337 number of single-crystal ages, thus their component analyses do not result in a reliable image  
338 on the substantive age components of the entire volcanic activity. That is why we evaluated  
339 the pooled data composed from the single-crystal ages of all samples from the Transdanubian  
340 Range by the component analysis methods. This pooled dataset does not contain the ages  
341 obtained on the distal "pietra verde" ash layers, as the aim of the dating and component  
342 analysis were to characterize the local volcanic sources. Two different algorithms were used  
343 to identify the age components: "PopShare" (Dunkl and Székely 2002) and "DensityPlotter"

344 (Vermeesch 2012). The former procedure assumes Gaussian distribution of the age  
345 components and uses the simplex algorithm (Cserepes 1989), while the "Density Plotter" uses  
346 the normal mixture modelling algorithm of Galbraith (2005). Beyond the Triassic age  
347 components Paleogene and Permian age components were also isolated from the Eocene  
348 conglomerates, but these are not in the scope of the current study. The Triassic age spectra  
349 could be decomposed to two major age components (Fig. 8). The two procedures resulted in  
350 identical mean values:  $238.1 \pm 4.0$  (s.d.) and  $238.2 \pm 0.9$  (s.e.) for the older, and  $228.1 \pm 3.4$   
351 (s.d.) and  $229.4 \pm 1.1$  (s.e.) for the younger age component ("PopShare" and "DensityPlotter",  
352 respectively). The isolated older age component corresponds to the younger TIMS ages of the  
353 "pietra verde" ash layers (e.g. Pálffy et al. 2003; Mundil et al. 2010; Wotzlav et al. 2018) and  
354 indicates that coarse-grained younger volcanoclastic sediments contain reworked fragments  
355 also from this slightly older volcanic event. The younger age component is an obvious proof  
356 on a distinct period of volcanic activity in Carnian time.

357

## 358 **Discussion**

359

360 The dikes and pebbles are mineralogically and chemically strongly transformed, thus the  
361 petrographical character of the volcanic rocks should be deduced mostly from the preserved  
362 mineral assemblages. The spectrum is wide, beyond quartz and K-feldspar both calcic and  
363 sodic plagioclase occur, and the mafic minerals reflect also the highly variable composition:  
364 olivine, pyroxene, amphibole and biotite were recognised. Only andesite dikes were hit by the  
365 deep drillings and exposed in the quarries, and in the pebbles and cobbles the most dominant  
366 lithologies are andesite, basaltic andesite, latite-trachyte, rhyolite and rhyolite tuff. One should  
367 consider the selective decomposition; the preserved pebble spectra are biased by the loss of

368 mechanically and chemically more sensitive lithologies like weakly welded tuffs and foid-  
369 bearing rocks.

370 A part of the volcanic rocks have altered chemical composition, as shown by the elevated LOI  
371 and the large variation in alkaline contents. In addition, even the relatively immobile HFS  
372 trace elements appear to show some secondary modification which makes the rock  
373 classification difficult. Nevertheless, most of the analysed samples can be classified as  
374 andesites based on fluid-immobile incompatible trace element ratios. The classification of the  
375 silicic volcanic rocks is more problematic, since fractionation of accessory minerals strongly  
376 affects these element ratios. The revised Th/Yb – Ta/Yb diagram (Gorton and Schandl, 2000  
377 after Pearce 1982, 1983) is used to infer the tectonic affinity of the volcanic rocks. All of them  
378 fall into the active continental margin field based on the relatively low Ta/Yb ratios. This  
379 geochemical character is similar to the rocks from the Dolomites (Castellarin et al. 1988) and  
380 confirm their common petrogenesis. According to our point of view the negative Nb-Ta  
381 anomaly in the trace element pattern and thus a lower Ta/Yb ratio could also originate from  
382 lithospheric mantle metasomatized by subduction related fluids in the past and remobilization  
383 during a lithospheric extension event (Sloman 1989 and Bonadiman et al. 1994). Together  
384 with the presence of the dikes penetrating platform carbonate and basinal carbonate  
385 successions, the abundance and large size of the Triassic volcanic pebbles and cobbles  
386 indicates that their source was within the Transdanubian Range. Long transport distance is not  
387 a plausible scenario for the provenance of the pebbles. A longer river could not develop on the  
388 passive margin that was dominated by the patchy arrangement of carbonate reefs and basins.  
389 Longer, wave-driven sediment transport alongshore or between the reef bodies is also not a  
390 feasible scenario due to the coarse size and partly angular shape of the detritus and the  
391 sensitivity of the volcanic lithologies to weathering. Pebbles of intrusive rocks are present  
392 only in minor amount in the Triassic and in the Eocene conglomerates, thus we assume a



393 volcanic centre, but the intrusive-subvolcanic root is less developed than in the case of the  
394 Predazzo Complex, or the erosion has not exhumed the subvolcanic level yet.  
395 The new U–Pb ages indicate that in the Transdanubian Range the deposition of the Anisian–  
396 Ladinian "pietra verde" tuff was followed by Carnian volcanism with variable, mafic to acid  
397 character. Remarkable, that the Triassic volcanoclastic successions in the central and eastern  
398 Southern Alps (Garzanti 1985) do not contain a distinct Carnian age group. The youngest U–  
399 Pb data of Beltrán-Triviño et al. (2013) form just a diffuse tail of "pietra verde" age  
400 components. Our U–Pb ages from the Eisenkappel granite confirms its Carnian emplacement  
401 age. As these ages are missing from the siliciclastic formations studied by Beltrán-Triviño et  
402 al. (2013) we can assume that this pluton was not yet exhumed to the surface and eroded in  
403 the Triassic or its contribution in the sediment was strongly diluted due to its minor size.  
404 Outside of eastern Southern Alps Carnian U–Pb ages or age components around 235–220 Ma  
405 were reported in the western Southern Alps (Crisci et al. 1984; Cassinis et al. 2008; Zanetti et  
406 al. 2013), in the Dinarides (Neubauer et al. 2014), in the Bükk Mountains (Haas et al. 2011;  
407 Kövér et al. 2018) and in Asia Minor in clastic sediments and also in a rhyolitic–andesitic  
408 volcanic succession (e.g. Ustaömer et al. 2016; Özdamar et al. 2013).  
409 It is useful to consider the actinide content of the dated zircons as a kind of diagnostic "proxy"  
410 for provenance purposes. The U content and the Th/U ratio of the dated zircon crystals  
411 indicate an obvious difference between the Triassic volcanic rocks of the Transdanubian  
412 Range and the pilot samples from the Southern Alps (Fig. 9). Thus, the immediate derivation  
413 of the volcanic pebbles found in the Transdanubian Range the silicic formations of Predazzo  
414 and Eisenkappel is rather unlikely.

415

## 416 **Conclusions**

417

418 - The presence of dikes and the proximal volcanoclastic material indicate volcanic eruptions in  
419 the Transdanubian Range in the Middle to Late Triassic.

420 - The composition of volcanic products covers a wide range from basalt to rhyolite. Although  
421 andesites are common, it is possible that the character of volcanism is bimodal, but the  
422 selective weathering/alteration biases the initial lithological variation. Volcanic textures are  
423 dominating, the intrusive and subvolcanic lithologies are scarce among the pebbles.

424 - The character of the igneous activity in the Transdanubian Range is similar to the South  
425 Alpine one. The local half-graben basins developed coevally with the volcanism indicating  
426 that the trigger of the magmatism was the extensional tectonics affecting the passive margin  
427 of the Adria plate, however their geochemistry shows also active margin character.

428 - Zircon U–Pb ages were determined on andesite dikes, tuff layers and on variable volcanic  
429 fragments from different clastic sediments. The sample-mean ages are between 239 and 228  
430 Ma. We could identify two age components by the evaluation of the pooled single-grain ages  
431 determined on detrital zircons and on pebble-population samples. Thus the volcanoclastic  
432 formations records two major periods of activity of zircon-bearing volcanism at 238 Ma and  
433 around 229–228 Ma, indicating well the presence Carnian magmatic activity within the  
434 Transdanubian Range.

435 - The geochemical character of the dated zircons differs from the composition of the zircon  
436 pilot samples from the Dolomites and Carnic Alps, and that rules out the origin of the pebbles  
437 and cobbles from the sensu stricto South Alpine igneous formations.

438 - The new zircon U–Pb age of the Eisenkappel granite approves the formerly published  
439 titanite U–Pb age and thus the emplacement age can be considered also as Carnian.

440

441 **References**

- 442 Armienti P, Corazzato C, Groppelli G, Natoli E, Pasquarè G (2003) Geological and  
443 petrographical study of Montecampione Triassic subvolcanic bodies (Southern Alps,  
444 Italy): preliminary geodynamic results. *Bollettino della Società geologica italiana*,  
445 spec vol 2:67-78
- 446 Balogh K, Németh K (2005) Evidence for the Neogene small-volume intracontinental  
447 volcanism in western Hungary; K/Ar geochronology of the Tihany Maar volcanic  
448 complex. *Geologica Carpathica* 56:91-99
- 449 Balogh K, Árvai-Sós E, Buda Gy (1983) Chronology of granitoid and metamorphic rocks of  
450 Transdanubia (Hungary). *Anuarul Institutului de Geologie și Geofizică* 61:359-364
- 451 Bébien, J, Blanchet R, Cadet J-P, Charvet J, Chorowicz J, Lapierre, H, Rampnoux J-P (1978)  
452 Middle Triassic volcanism in the Dinarides of Yugoslavia: its place in the peri-  
453 Mediterranean geotectonic evolution (Le volcanisme triasique des Dinarides en  
454 Yougoslavie: SA place dans l'évolution géotectonique péri-méditerranéenne, in French  
455 with English abstract). *Tectonophysics* 47:159-176
- 456 Bechstädt T, Mostler H (1976) Middle-Triassic reef-basin-development in the western part of  
457 the Northern Limestone Alps (Riff-Becken-Entwicklung in der Mitteltrias der  
458 westlichen Nördlichen Kalkalpen, in German with English abstract). *Zdt. Geol. Ges.*  
459 127:271-289
- 460 Beltrán-Triviño A, Winkler W, von Quadt A (2013) Tracing Alpine sediment sources through  
461 laser ablation U-Pb dating and Hf-isotopes of detrital zircons. *Sedimentology* 60:197-  
462 224
- 463 Beltrán-Triviño A, Winkler W, von Quadt A, Gallhofer D (2016) Triassic magmatism on the  
464 transition from Variscan to Alpine cycles: evidence from U-Pb, Hf, and geochemistry  
465 of detrital minerals. *Swiss Journal of Geosciences* 109:309-328

- 466 Bertotti G, Picotti V, Bernoulli D, Castellarin A (1993) From rifting to drifting: tectonic  
467 evolution of the South-Alpine upper crust from the Triassic to the Early Cretaceous.  
468 *Sedimentary Geology* 86:53-76
- 469 Blendinger W (1984) Late Ladinian strike-slip tectonics of the Marmolada-Costabella area  
470 (Dolomites). *Jahrbuch Geologische Bundesanstalt B-A, Wien*, 127:307-319
- 471 Böckh J (1873) The geological conditions of the southern part of the Bakony I (Die  
472 geologischen Verhältnisse des südlichen Theiles des Bakony, I, in German).  
473 *Mittheilungen aus dem Jahrbuche der königlichen ungarischen geologischen Anstalt*, 2  
474 (2): 27-182
- 475 Bonadiman C, Coltorti M, Siena F (1994) Petrogenesis and T-fO<sub>2</sub> estimates of Mt. Monzoni  
476 complex (Central Dolomites, Southern Alps): a Triassic shoshonitic intrusion in a  
477 transcurrent geodynamic setting. *European Journal of Mineralogy* 6:943-966
- 478 Borsi S, Ferrara G (1967) Age determination of the intrusive rocks of Predazzo with Rb/Sr  
479 and K/Ar methods (Determinazione dell'età delle rocce intrusive di Predazzo con i  
480 metodi del Rb/Sr e K/Ar, in Italian with English Abstract). *Mineralogica et*  
481 *Petrographica Acta* 14:171-183
- 482 Borsi S, Ferrara G, Paganelli L, Simboli G (1968) Isotopic age measurements of the M.  
483 Monzoni intrusive complex. *Mineralogica et Petrographica Acta* 14:171-183
- 484 Bosellini A, Gianolla P, Stefani M (2003) Geology of the Dolomites. *Episodes* 26:181-185
- 485 Brack P, Rieber H, Nicora A, Mundil R (2005) The Global boundary Stratotype Section and  
486 Point (GSSP) of the Ladinian Stage (Middle Triassic) at Bagolino (Southern Alps,  
487 Northern Italy) and its implications for the Triassic time scale. *Episodes* 28:233-244
- 488 Budai T, Vörös A (1993) The Middle Triassic events of the Transdanubian Central Range in  
489 the frame of the Alpine evolution. *Acta Geologica Hungarica* 36:3-13

490 Budai T, Vörös A (2006) Middle Triassic platform and basin evolution of the Southern  
491 Bakony mountains (Transdanubian Range, Hungary). *Rivista Italiana di Paleontologia*  
492 *e Stratigrafia* 112:359-371

493 Budai T, Császár G, Csillag G, Dudko A, Koloszar L, Majoros Gy (1999) Geology of the  
494 Balaton Highland : explanation to the Geological map of the Balaton Highland, 1:50  
495 000., Geological Institute of Hungary

496 Budai T, Csillag G, Vörös A, Lelkes Gy (2001) Middle to Late Triassic platform and basin  
497 facies of the Eastern Bakony Mts. (Transdanubian Range, Hungary). *Bulletin of the*  
498 *Hungarian Geological Society* 131:71-95

499 Budai T, Németh K, Piros O (2005) Middle Triassic platform carbonates and volcanites in the  
500 Latemar area (Dolomites, Italy). *Annual Report of the Geological Institute of Hungary*  
501 *on year 2004: 175-188*

502 Budai T, Haas J, Piros O (2015) New stratigraphic data on the Triassic basement of the  
503 Zsámbék Basin - tectonic inferences. *Bulletin of the Hungarian Geological Society*  
504 145:247-257

505 Carraro A, Visonà D (2003) Mantle xenoliths in Triassic camptonite dykes of the Predazzo  
506 Area (Dolomites, Northern Italy): petrography, mineral chemistry and  
507 geothermobarometry. *European Journal of Mineralogy* 15:103-115

508 Casetta F, Coltorti M, Marrocchino E (2018) Petrological evolution of the Middle Triassic  
509 Predazzo Intrusive Complex, Italian Alps. *International Geology Review* 60:977-997

510 Cassinis G, Cortesogno L, Gaggero L, Perotti CR, Buzzi L (2008) Permian to Triassic  
511 geodynamic and magmatic evolution of the Brescian Prealps (eastern Lombardy,  
512 Italy). *Boll Soc Geol It* 127:501-518

513 Castellarin A, Rossi RML (1981) The Southern Alps: an aborted Middle Triassic mountain  
514 chain? *Ecl Geol Helv* 74:313-316

- 515 Castellarin A, Lucchini IF, Rossi PL, Selli L, Simboli G (1988) The Middle Triassic  
516 magmatic-tectonic arc development in the Southern Alps. *Tectonophysics* 146:79-89
- 517 Cohen KM, Finney SC, Gibbard PL, Fan J-X (2013; updated) The ICS International  
518 Chronostratigraphic Chart. *Episodes* 36:199-204  
519 <http://stratigraphy.org/ICSchart/ChronostratChart2017-02.pdf>. Accessed February  
520 2017
- 521 Crisci GM, Ferrara G, Mauzzoli R, Rossi PM (1984) Geochemical and geochronological data  
522 on Triassic volcanism of the Southern Alps of Lombardy (Italy): Genetic implications.  
523 *Geol Rundschau* 73:279-292
- 524 Cros E, Szabó I (1984) Comparison of the Triassic volcanogenic formations in Hungary and  
525 in the Alps. Paleogeographic criteria. *Acta Geologica Hungarica* 27:265-276
- 526 Cserepes L (1989) Numerical mathematics - for geophysicist students (in Hungarian).  
527 Tankönyvkiadó, Budapest
- 528 Csontos L, Vörös A (2004) Mesozoic plate tectonic reconstruction of the Carpathian region.  
529 *Paleogeography Paleoclimatology Paleoecology* 210:1-56
- 530 Dosztály L (1993) The Anisian/Ladinian and Ladinian/ Carnian boundaries in the Balaton  
531 Highland based on Radiolarians. *Acta Geologica Hungarica* 36: 59-72
- 532 Dunkl I, Horváth I, Józsa S (2003) Andesite dikes and skarn formations of Szár Hill, Polgárdi,  
533 Hungary. In: Szakáll S, Fehér B (eds) *Minerals of Szár Hill*. Herman Ottó Museum,  
534 Miskolc, pp 55-86, (in Hungarian)
- 535 Dunkl I, Frisch W, Kuhlemann J, Brügel A (2009) Pebble population dating as an additional  
536 tool for provenance studies - examples from the Eastern Alps. Geological Society,  
537 London, Special Publications 324:125-140

538 Dunkl I, Székely B (2002) Component analysis of detrital FT ages - with visualization of the  
539 fitting. Salamanca, International Workshop on Fission Track Analysis, Cádiz, 4-7 June  
540 2002. *Geotemas* 4:63

541 Dunkl I, Mikes T, Simon K, von Eynatten H (2008) Brief introduction to the Windows  
542 program Pepita: data visualization, and reduction, outlier rejection, calculation of trace  
543 element ratios and concentrations from LA-ICP-MS data. In: Sylvester P (ed) *Laser  
544 ablation ICP-MS in the Earth Sciences: Current practices and outstanding issues.*  
545 *Mineralogical Association of Canada, Short Course* 40:334-340

546 Farics É, Józsa S (2017) Petrographic investigation of the Triassic volcanogenic formations of  
547 the Eastern Bakony and interpretation of their genesis (in Hungarian with English  
548 abstract). *Földtani Közlöny, Bulletin of the Hungarian Geological Society* 147:25-38

549 Farics É, Józsa S, Haas J (2015) Petrographic features of lava rock and tuff clast-bearing  
550 sedimentary rocks at the base of the Upper Eocene succession in the Buda Hills.  
551 *Földtani Közlöny, Bulletin of the Hungarian Geological Society* 145:331-350

552 Ferrara G, Innocenti F (1974) Radiometric age evidence of a Triassic thermal event in the  
553 Southern Alps. *Geologische Rundschau* 63:572-581

554 Frei D, Gerdes A (2009) Precise and accurate in situ U-Pb dating of zircon with high sample  
555 throughput by automated LA-SF-ICP-MS. *Chemical Geology* 261:261-270

556 Furrer H, Schaltegger U, Ovtcharova M, Meister P (2008) U-Pb zircon age of volcanoclastic  
557 layers in Middle Triassic platform carbonates of the Austroalpine Silvretta nappe  
558 (Switzerland). *Swiss Journal of Geosciences* 101:595-603

559 Gaetani M, Fois E, Jadoul F, Nicora A (1981) Nature and evolution of Middle Triassic  
560 carbonate Buildup in the Dolomites (Italy). *Marine Geology* 44:25-57

561 Galbraith RF (2005) *Statistics for Fission Track Analysis.* Chapman and Hall/CRC,  
562 *Interdisciplinary Statistics Series, London*

563 Gallitelli P, Simboli G (1971) Petrological and Geochemical Research on the Rocks of  
564 Predazzo and Monzoni (North Italy). *Verhandlungen der Geologischen Bundesanstalt*  
565 2:326-343, Vienna

566 Garzanti E (1985) The sandstone memory of the evolution of a Triassic volcanic arc in the  
567 Southern Alps, Italy. *Sedimentology* 32:423-433

568 Gorton MP, Schandl ES (2000) From continents to island arcs: a geochemical index of  
569 tectonic setting for arc-related and within-plate felsic to intermediate volcanic rocks.  
570 *Canadian Mineralogist* 38:1065-1073

571 Haas J (2013) *Geology of Hungary*, Springer

572 Haas J, Budai T (1995) Upper Permian–Triassic facies zones in the Transdanubian Range.  
573 *Rivista Italiana Paleontologia Stratigrafia* 101:249-266

574 Haas J, Kovács S, Krystyn L, Lein R (1995) Significance of Late Permian-Triassic facies  
575 zones in terrane reconstructions in the Alpine-North Pannonian domain.  
576 *Tectonophysics* 242:19-40

577 Haas J, Budai T, Csontos L, Fodor L, Konrád Gy (2010) Magyarország pre-kainozoos  
578 földtani térképe 1:500000 (Pre-Cenozoic geological map of Hungary, 1:500000).  
579 Hungarian Geological Survey, Budapest.

580 Haas J, Kovács S, Pelikán P, Kövér Sz, Görög Á, Ozsvárt P, Józsa S, Németh N (2011)  
581 Remnants of the accretionary complex of the Neotethys Ocean in Northern Hungary.  
582 *Földtani Közlöny, Bulletin of the Hungarian Geological Society* 141:412-66

583 Haas J, Budai T, Dunkl I, Farics É, Józsa S, Kövér Sz, Götz AE, Piros O, Szeitz P (2017) The  
584 Budaörs–1 well revisited: Stratigraphic and tectonic implications. *Central European*  
585 *Geology*. <https://doi.org/10.1556/24.60.2017.008>



586 Harangi Sz, Szabó Cs, Józsa S, Szoldán Zs, Árva-Sós E, Balla M, Kubovics I (1996)  
587 Mesozoic igneous suites in Hungary: Implications for genesis and tectonic setting in  
588 the northwestern part of Tethys. *International Geology Review* 38:336-360

589 Horváth E, Tari G (1987) Middle Triassic volcanism in the Buda Mountains. *Annales*  
590 *Universitatis Scientiarum Budapestiensis de Rolando Eötvös Nominatae, Sect Geol*  
591 27:3-16

592 Jackson S, Pearson N, Griffin W, Belousova E (2004) The application of laser ablation-  
593 inductively coupled plasma-mass spectrometry to in situ U-Pb zircon geochronology.  
594 *Chemical Geology* 211:47-69

595 Jelaska V, Kolar-Jurkovšek T, Jurkovšek B, Grušić I (2003) Triassic beds in the basement of  
596 the Adriatic-Dinaric carbonate platform of Mt. Svilaja (Croatia). *Geologija* 46:225-  
597 230

598 Kázmér M, Kovács S (1985) Permian–Paleogene paleogeography along the eastern part of the  
599 Insubric–Periadriatic lineament system: evidence for continental escape of the  
600 Bakony–Drauzug unit. *Acta Geologica Hungarica* 28:71-84

601 Kiss J (1954) Andesite from Szabadbattyán and its importance concerning the genesis of ores  
602 (Szabadbattyáni andezit és ércgenetikai jelentősége, in Hungarian with English  
603 abstract). *Földtani Közlöny, Bulletin of the Hungarian Geological Society* 84:183-189.

604 Kovács S (1994) Conodonts of stratigraphical importance from the Anisian/Ladinian  
605 boundary interval of the Balaton Highland, Hungary. *Rivista Italiana di Paleontologia*  
606 *e Stratigrafia* 99: 473-514

607 Kövér S, Fodor L, Kovács Z, Klötzli U, Haas J, Zajzon N, Szabó C. (2018) Late Triassic  
608 acidic volcanic clasts in different Neotethyan sedimentary mélanges: paleogeographic  
609 and geodynamic implications. *International Journal of Earth Sciences* 107:2975-2998

610 Kubovics I (1985) Mesozoic magmatism of the Transdanubian Mid-Mountains. *Acta*  
611 *Geologica Hungarica* 28:141-164

612 Laurenzi MA (1994) High resolution Ar/Ar chronology of Predazzo magmatic complex  
613 (Southern Alps, Italy). US. Geological Survey, circular 1107, ICOG pp 8

614 Leake BE, Wolley AR, Arps CES, Birch WD, Gilbert MC, Grice JD, Hawthorne FC, Kato A,  
615 Kisch HJ, Krivovichev VG, Linthout K, Laird J, Mandarino J (1997) Nomenclature of  
616 Amphiboles: Report of the Subcommittee on Amphiboles of the International  
617 Mineralogical Association Commission on New Minerals and Mineral Names.  
618 *Mineralogical Magazine* 61:295-321

619 Le Bas MJ, Le Maitre RW, Streckeisen A, Zanettin B (1986) A chemical classification of  
620 volcanic rocks based on the total alkali-silica diagram. *Journal of Petrology* 27:745-  
621 750

622 Lippolt HJ, Pidgeon R (1974) Isotopic mineral ages of a diorite from the Eisenkappel  
623 intrusion, Austria. *Z Naturforsch* 29a:966-968

624 Lóczy L (1916) The geology and tectonics of the Balaton Highland (Die geologische  
625 Formationen der Balatongegend und ihre regionale Tektonik, in German). In:  
626 *Resultate der wissenschaftlichen Erforschung des Balatonsees* 1, pp 716

627 Lucchini F, Rossi PL, Simboli G (1982) Triassic magmatism in the Predazzo area (Il  
628 *magmatismo triassico dell'area di Predazzo*, in Italian). In: Castellarin A, Vai GB  
629 (eds) *Guida alla Geologia del Sudalpino centro-orientale*. Società Geologica Italiana,  
630 *Guide Geologiche Regionali*, Roma, pp 221-229

631 Ludwig KR (2012) User's manual for Isoplot 3.75: A geochronological Toolkit for Microsoft  
632 Excel. Berkeley Geochronology Center Special Publication 4:70

633 Márton E, Budai T, Haas J, Kovács J, Szabó I, Vörös A (1997) Magnetostratigraphy and  
634 biostratigraphy of the Anisian–Ladinian boundary section Felsőörs (Balaton Highland,  
635 Hungary). *Albertiana* 20:50-57

636 McDonough WF, Sun S (1995) The composition of the Earth. *Chemical Geology* 120:223-  
637 253

638 Menegazzo Vitturi L, Visonà D, Zantedeschi C (1995) Amphibole composition of Predazzo  
639 volcano-plutonic complex (Southern Alps, Italy) *Sciences Géologiques – Memoires*.  
640 47:87-94

641 Miller C, Thöni M, Goessler W, Tessadri R (2011) Origin and age of the Eisenkappel gabbro  
642 to granite suite (Carinthia, SE Austrian Alps). *Lithos* 125:434-448

643 Mojsisovics E (1879) The dolomite reefs of South Tyrol and Veneto: contributions to the  
644 development of the Alps (Die Dolomit-Riffe von Südtirol und Venetien: Beiträge zur  
645 Bildungsgeschichte der Alpen, in German). Wien, Hölder

646 Morimoto N (1988) Nomenclature of pyroxenes. *Mineralogy and Petrology* 39:55-76

647 Mundil R, Brack P, Meier M, Rieber H, Oberli F (1996) High resolution U-Pb dating of  
648 middle Triassic volcanoclastics: time-scale calibration and verification of tuning  
649 parameters for carbonate sedimentation. *Earth and Planetary Science Letters* 141:137-  
650 151

651 Mundil R, Pálffy J, Renne PR, Brack P (2010) The Triassic timescale: new constraints and a  
652 review of geochronological data. In: Lucas SG (ed) *The Triassic Timescale*. Special  
653 Publications, Geological Society (London) 334:41-60

654 Németh K, Budai T (2009) Diatremes cut through the Triassic carbonate platforms in the  
655 Dolomites? Evidences from and around the Latemar, Northern Italy. *Episodes* 32:74-  
656 83

657 Neubauer F, Xiaoming L, Borojević Šoštarić S, Bianca H, Yunpeng D (2014) U-Pb zircon  
658 data of Middle-Upper Triassic magmatism in Southern Alps and NW Dinarides:  
659 Implications for the Southeast Mediterranean tectonics. Buletini i Shkencave  
660 Gjeologjike, Proceedings XX Congress of the Carpathian-Balkan Geological  
661 Association, Tirana, Albania

662 Obenholzner JH (1991) Triassic volcanogenic sediments from the Southern Alps (Italy,  
663 Austria, Yugoslavia) - a contribution to the "Pietra verde" problem. *Sedimentary  
664 Geology* 74:157-171

665 Özdamar S, Billor MZ, Sunal G, Esenli F, Roden MF (2013) First U-Pb SHRIMP zircon and  
666  $^{40}\text{Ar}/^{39}\text{Ar}$  ages of metarhyolites from the Afyon-Bolkardag Zone, SW Turkey:  
667 Implications for the rifting and closure of the Neo-Tethys. *Gondwana Research  
668* 24:377-391

669 Paces JB, Miller JD (1993) Precise U-Pb ages of Duluth Complex and related mafic  
670 intrusions, northeastern Minnesota: geochronological insights into  
671 physical, petrogenetic, paleomagnetic and tectonomagmatic processes associated with  
672 the 1.1 Ga midcontinent rift system. *Journal of Geophysical Research* 98:13997-14013

673 Pálffy J, Parrish RR, David K, Vörös A (2003) Middle Triassic integrated U-Pb  
674 geochronology and ammonoid biochronology from the Balaton Highland (Hungary)  
675 *Journal of the Geological Society (London)* 160:271-284

676 Pearce JA (1982) Trace elements characteristics of lavas from destructive plate boundaries.  
677 In: Thorpe RS (ed) *Andesites*. Wiley, New York, N.Y., pp. 525-548

678 Pearce JA (1983) Role of the sub-continental lithosphere in magma genesis at active  
679 continental margins. In: Hawkesworth CJ, Norry MJ (eds) *Continental Basalts and  
680 Mantle Xenoliths*. Shiva, Nantwich, pp. 230-249

681 Pearce J A (1996) A Users guide to basalt discrimination diagrams. In: Wyman DA (ed)  
682 Trace element geochemistry of volcanic rocks: Applications for massive sulphide  
683 exploration 12, Geol. Ass. Canada Short Course Notes, pp. 79-113

684 Preto N, Hinnov LA, Hardie LA, De Zanche V (2001) Middle Triassic orbital signature  
685 recorded in the shallow-marine Latemar carbonate buildup (Dolomites, Italy) *Geology*  
686 29:1123-1126

687 Putiš M, Kotov AB, Uher P, Salnikova JB, Korikovsky SP (2000) Triassic age of the Hrončok  
688 Pre-Orogenic A-type granite related to continental rifting: A new result of U-Pb  
689 isotope dating (Western Carpathians). *Geologica Carpathica* 51:59-66

690 Raincsák Gy (1980) The structure of the Triassic formations at Várpalota-Iszkaszentgyörgy.  
691 Annual Report of the Geological Institute of Hungary 1978:187-196

692 Ravasz Cs (1973) Mineralogical-petrographical studies on Middle Triassic tuffs of the  
693 Transdanubian Central Mountains, Hungary. *Acta Mineralogica Petrographica*, Szeged  
694 21:123-139

695 Schmid SM, Bernoulli D, Fügenschuh B, Matenco L, Schefer S, Schuster R, Tischler M,  
696 Ustaszewski K (2008) The Alpine-Carpathian-Dinaride-orogenic system: correlation  
697 and evolution of tectonic units. *Swiss Journal of Geosciences* 101:139-183

698 Sircombe KN (2004) AgeDisplay: an EXCEL workbook to evaluate and display univariate  
699 geochronological data using binned frequency histograms and probability density  
700 distributions. *Computers & Geosciences* 30:21-31

701 Sláma J, Košler J, Condon DJ, Crowley JL, Gerdes A, Hanchar JM, Horstwood MSA, Morris  
702 GA, Nasdala L, Norberg N, Schaltegger U, Schoene B, Tubrett MN, Whitehouse MJ  
703 (2008) Plešovice zircon - A new natural reference material for U-Pb and Hf isotopic  
704 microanalysis. *Chemical Geology* 249:1-35

705 Sloman LE (1989) Triassic shoshonites from the Dolomites, Northern Italy: alkaline rocks in  
706 a strike-slip setting. *Journal Geophysical Research* 94:4655-4666

707 Stockar R, Baumgartner PO, Condon D (2012) Integrated Ladinian bio-chronostratigraphy  
708 and geochronology of Monte San Giorgio (Southern Alps, Switzerland). *Swiss Journal*  
709 *of Geosciences* 105:85-108

710 Storck JC, Brack P, Wotzlaw JF, Ulmer P (2018) Timing and evolution of Middle Triassic  
711 magmatism in the Southern Alps (Northern Italy). *Journal of the Geological Society*,  
712 <https://doi.org/10.1144/jgs2018-123>

713 Szabó C et al. (1996) Mineralogy and geochemistry of magmatic rocks of Budafok-1 borehole  
714 (Budafok-1 (Bf-1) fúrás magmás összetételének ásványközettani és geokémiai vizsgálata,  
715 in Hungarian). Department of Petrology and Geochemistry, Eötvös Loránd University,  
716 Hungary, 27 p.

717 Szabó I, Ravasz Cs (1970) Investigation of the Middle Triassic volcanics of the  
718 Transdanubian Central Mountains, Hungary. *Ann Hist Natur Mus Nat Hung* 62:31-51

719 Szoldán Zs (1990) Middle Triassic magmatic sequences from different tectonic settings in the  
720 Bükk Mts., NE Hungary. *Acta Mineralogica-Petrographica, Szeged* 31:25-42

721 Tari G, Horváth E, Rumppler J (1992) Styles of extension in the Pannonian Basin.  
722 *Tectonophysics* 208:203-219

723 Ustaömer T, Ustaömer PA, Robertson AHF, Gerdes A (2016) Implications of U-Pb and Lu-  
724 Hf isotopic analysis of detrital zircons for the depositional age, provenance and  
725 tectonic setting of the Permian–Triassic Palaeotethyan Karakaya Complex, NW  
726 Turkey. *International Journal of Earth Sciences* 105:7-38

727 Velledits F (2006) Evolution of the Bükk Mountains (NE Hungary) during the Middle–Late  
728 Triassic asymmetric rifting of the Vardar-Meliata branch of the Neotethys Ocean.  
729 *International Journal of Earth Sciences* 95: 395-412

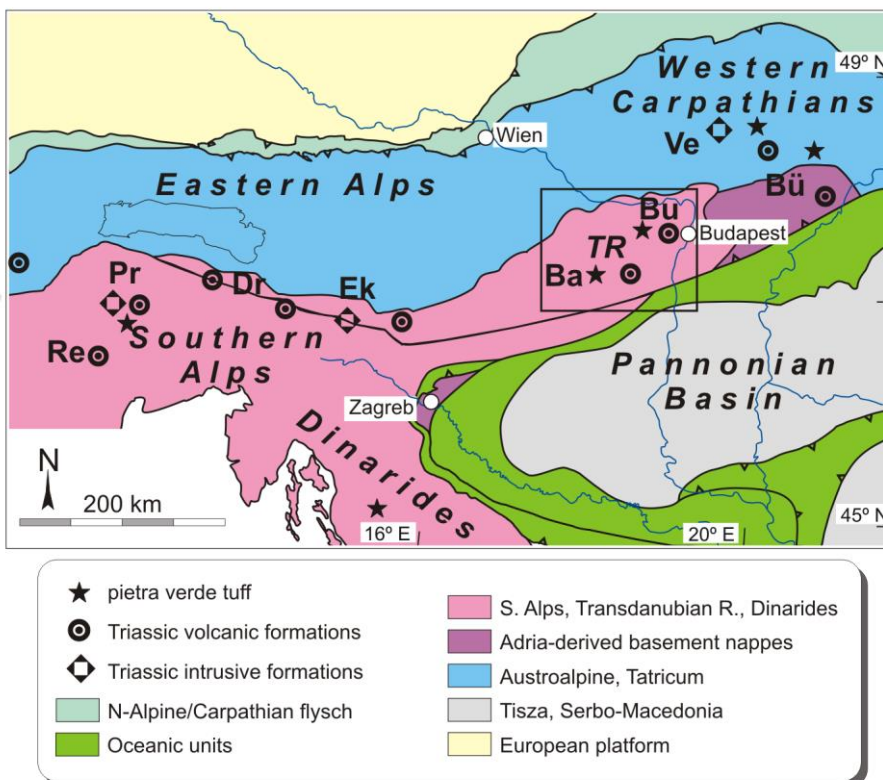
- 730 Vermeesch P (2012) On the visualisation of detrital age distributions. *Chemical Geology* 312-  
731 313:190-194
- 732 Visonà D (1997) The Predazzo multipulse intrusive body (Western Dolomites, Italy). *Field*  
733 *and mineralogical studies. Memorie di Scienze Geologiche* 49:117-125
- 734 Vörös A (1993) Redefinition of the Reitzi Zone at its type region (Balaton area, Hungary) as  
735 the basal zone of the Ladinian. *Acta Geologica Hungarica* 36:15-38
- 736 Vörös A (2000) The Triassic of the Alps and Carpathians and its interregional correlation. In:  
737 Hongfu Yin, Dickins JM, Shi GR, Jinnan Tong (eds) *Permian–Triassic Evolution of*  
738 *Tethys and Western Circum–Pacific. Elsevier, 412 p. [http://dx.doi.org/](http://dx.doi.org/10.1016/S0920-5446(00)80011-4)*  
739 *10.1016/S0920-5446(00)80011-4*
- 740 Vörös A, Szabó I, Kovács S, Dosztály L, Budai T (1996) The Felsőörs section: a possible  
741 stratotype for the base of the Ladinian stage. *Albertiana* 17:25-40
- 742 Vörös A, Budai T, Haas J, Kovács S, Kozur H, Pálffy J (2003) A proposal for the GSSP at the  
743 base of the Reitzi Zone (*sensu stricto*) at Bed 105 in the Felsőörs section, Balaton  
744 Highland, Hungary. *Albertiana* 28:35-47
- 745 Webb JA (1982) A Carnian age from the Mt. Monzoni intrusive complex, western Dolomites,  
746 Italy. In: Odin GS (ed) *Numerical dating in stratigraphy. Wiley, New York, pp 875-*  
747 *876*
- 748 Wein Gy (1977) *Tectonics of Buda Hills. Geological Institute of Hungary, Budapest, pp 76*
- 749 Wiedenbeck M, Allé P, Corfu F, Griffin WL, Meier M, Oberli F, von Quadt A, Roddick JC,  
750 Spiegel W (1995) Three natural zircon standards for U–Th–Pb, Lu–Hf, trace element  
751 and REE analyses. *Geostandards Newsletters* 19:1-23
- 752 Wotzlaw JF, Brack P, Storck JC (2018) High-resolution stratigraphy and zircon U–Pb  
753 geochronology of the Middle Triassic Buchenstein Formation (Dolomites, northern

754 Italy): precession-forcing of hemipelagic carbonate sedimentation and calibration of  
 755 the Anisian–Ladinian boundary interval. *Journal of the Geological Society* 175:71-85  
 756 Zanetti A, Mazzucchelli M, Sinigoi S, Giovanardi T, Peressini G, Fanning M (2013) SHRIMP  
 757 U-Pb zircon Triassic intrusion age of the Finero mafic complex (Ivrea-Verbano Zone,  
 758 Western Alps) and its geodynamic implications. *Journal of Petrology* 54:2235-2265

759

760 **Captions**

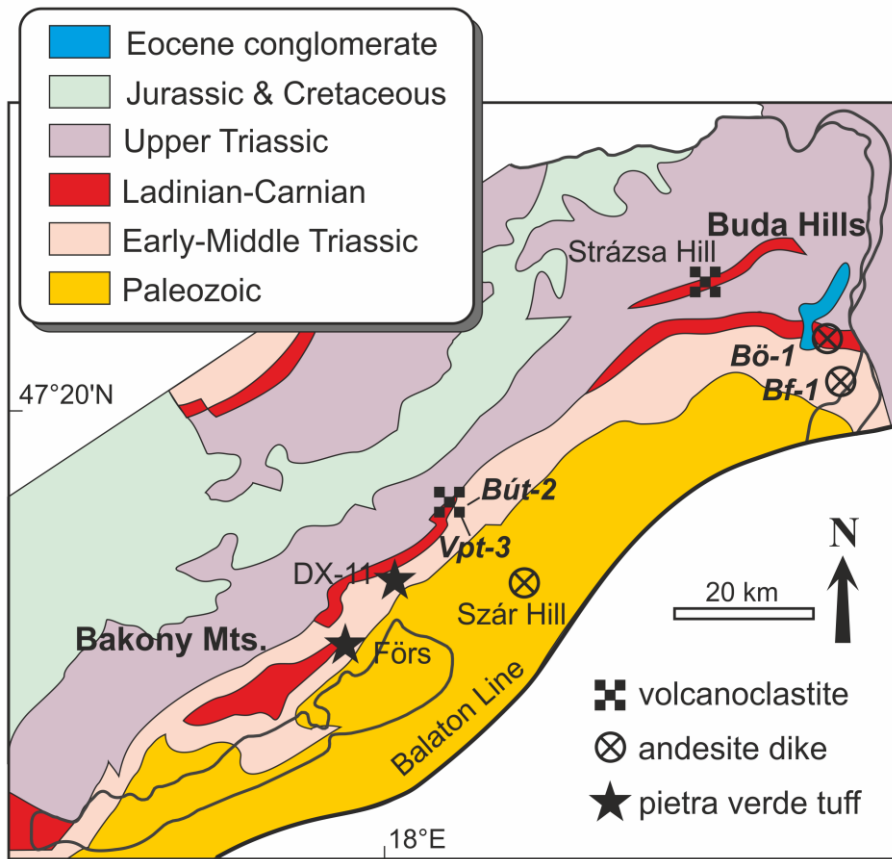
761 Figure 1: Simplified structural map of the Southern Alps, the Transdanubian Range (TR) and  
 762 the surrounding areas with the major occurrences of the Triassic igneous formations (map  
 763 base after Csontos and Vörös 2004; Schmid et al. 2008). Square represents the geological map  
 764 of TR (Fig. 2). Abbreviations of the most significant intrusive complexes and tuff/volcanic  
 765 occurrences: Re - Recoaro, Pr - Predazzo, Dr - Drauzug, Ek - Eisenkappel, Ba - Bakony Mts.,  
 766 Bu - Buda Hills, Bü - Bükk Mts., Ve - Vepor Mts.).



767



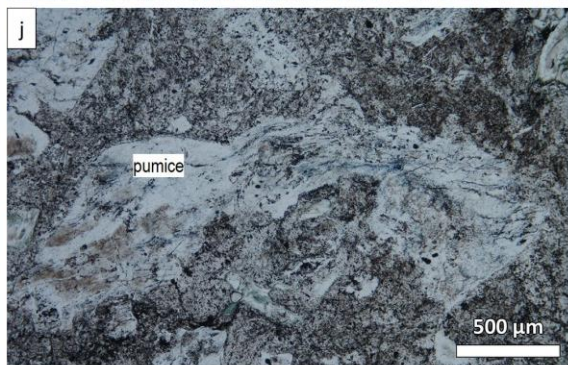
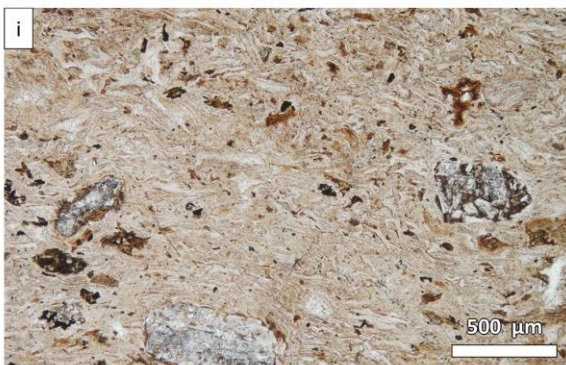
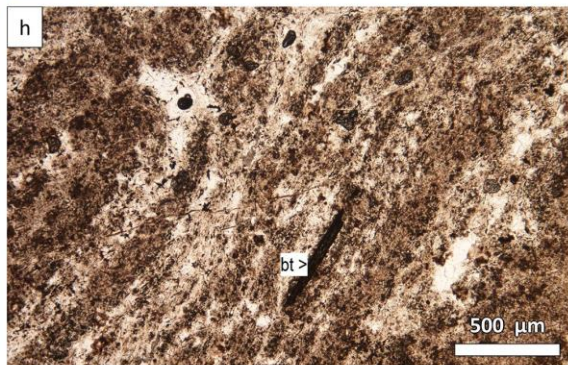
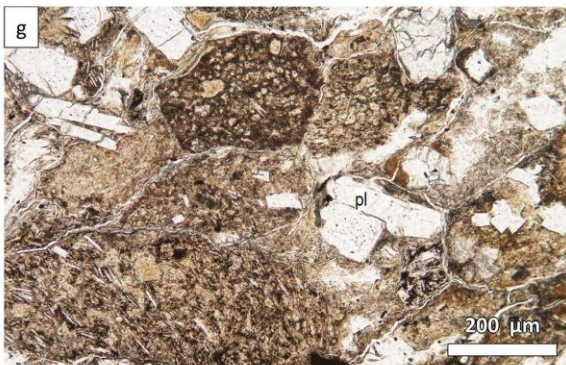
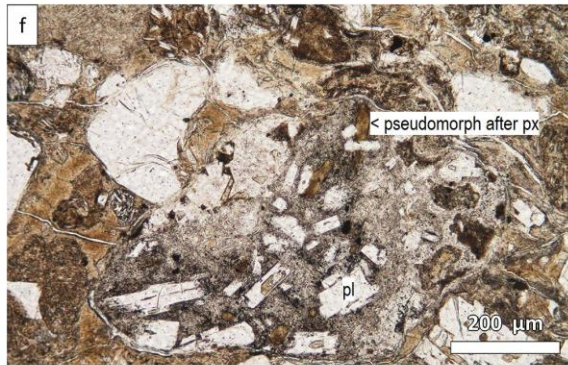
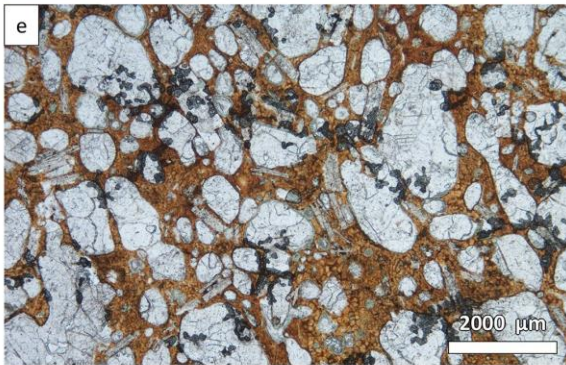
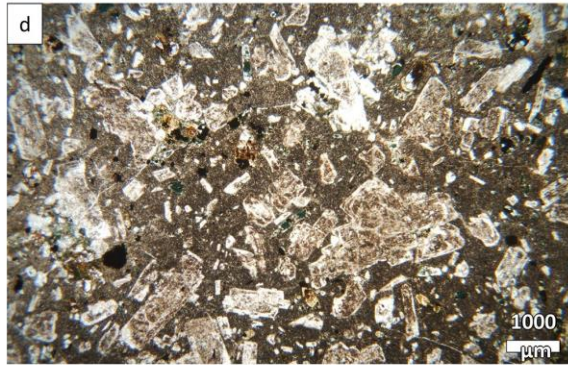
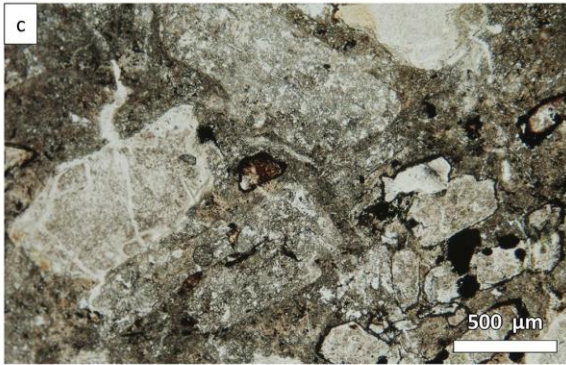
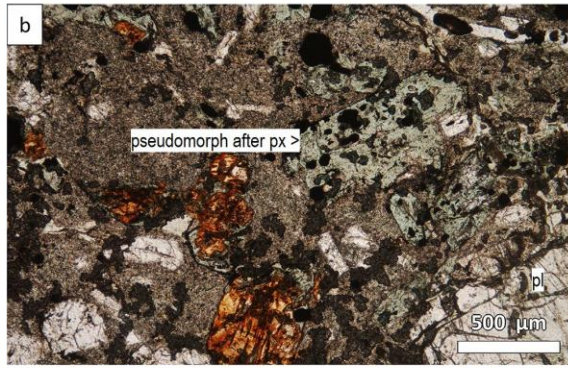
768 Figure 2: Simplified geological map of the Transdanubian Range without Cenozoic  
 769 sedimentary cover (after Haas et al. 2010). Codes of boreholes are in italics (for explanation  
 770 of abbreviations see Table 1).



771  
 772 Figure 3: Characteristic photomicrographs showing the textures of Middle-Late Triassic  
 773 volcanic rocks from the Transdanubian Range. Böt-1: Budaörs-1 borehole, Bút-2: Bakonykúti-  
 774 2 borehole; for the localities see Fig. 2.  
 775 a: Texture of fresh andesite (crossed N), Böt-1, 773 m (from Farics et al. 2015). b: Texture of  
 776 weakly altered andesite. The pyroxene is altered to secondary minerals, but the plagioclase is  
 777 fresh (1N), Böt-1, 775.9 m. c: Strongly altered andesite clast in Eocene conglomerate with  
 778 pseudomorphs of phenocrysts (1N), Budakeszi. d: Texture of K-trachyte - rims of K-feldspar  
 779 along altered plagioclase (by K-metasomatism) and pseudomorph after pyroxene (1N), Böt-1,  
 780 808.6 m. e: Strongly vesiculated texture of a basalt clast in the volcanogenic  
 781 sandstone/conglomerate (1N), Hideg Valley, Inota. f: Texture of andesite clast (1N), Bút-2, 62

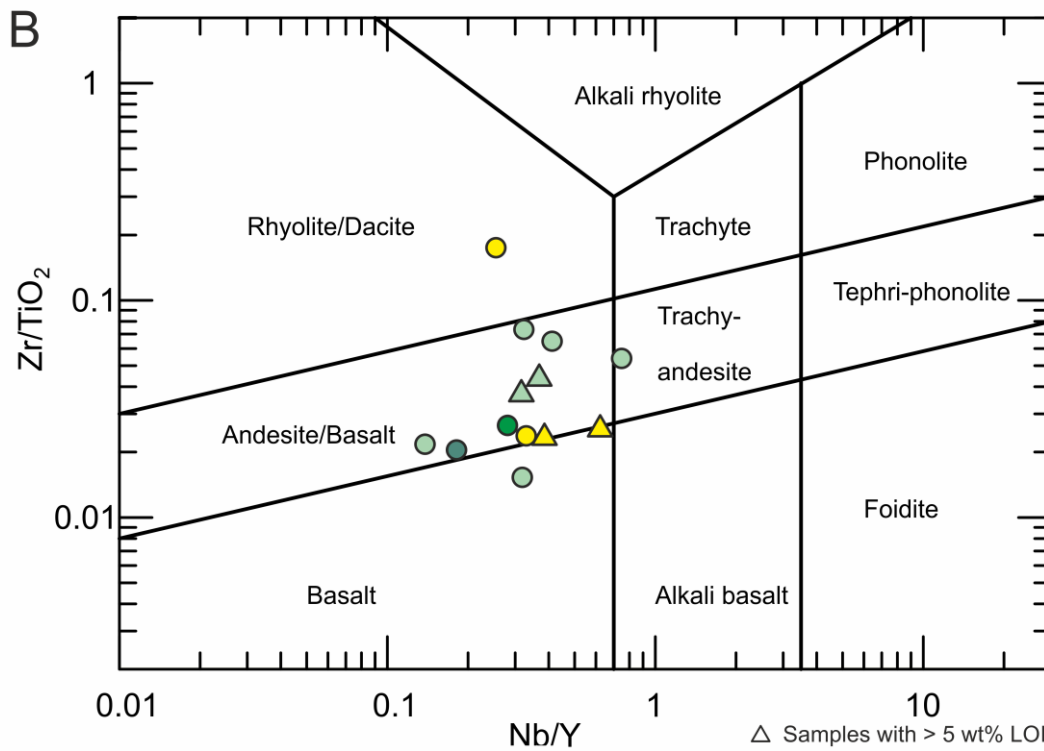
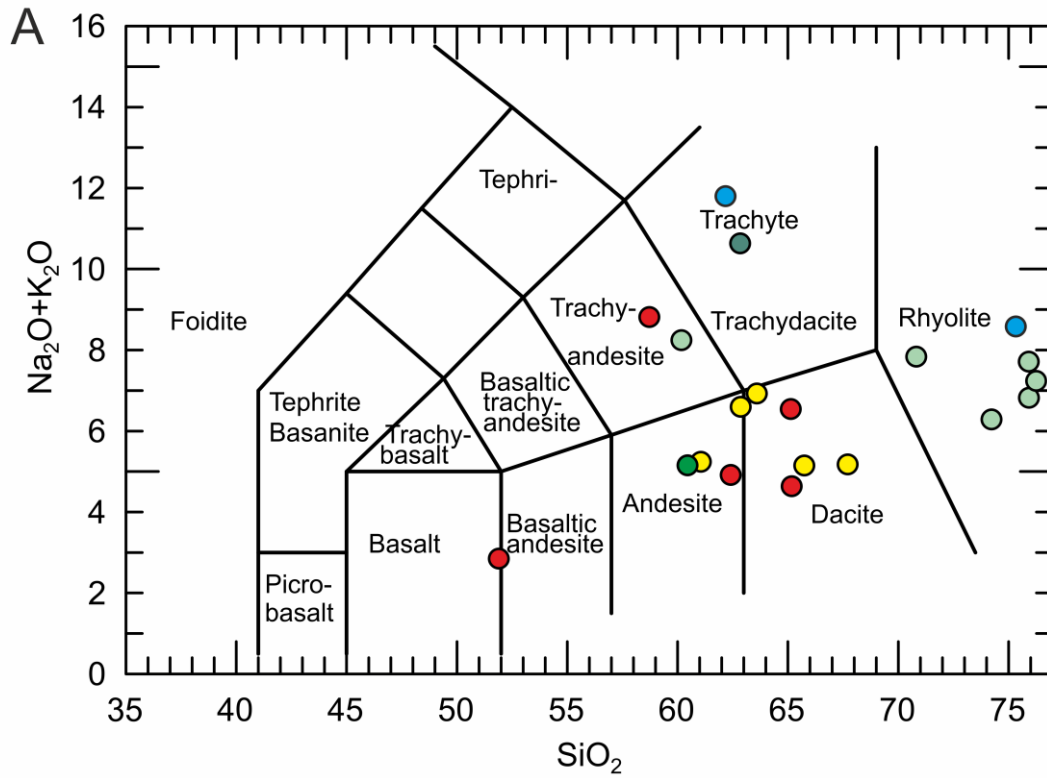
782 m (from Farics and Józsa 2017). g: Texture of basalt/andesite clasts in volcanogenic rock  
783 (1N), Bút-2 62 m. h: Texture of flow banding rhyolite clast (1N), Hideg Valley. i: Texture of  
784 moderately welded ignimbrite clast (1N), Strázsa Hill. j: Texture of acid tuff clast in Eocene  
785 conglomerate (1N), Kő Hill (Farics et al. 2015).





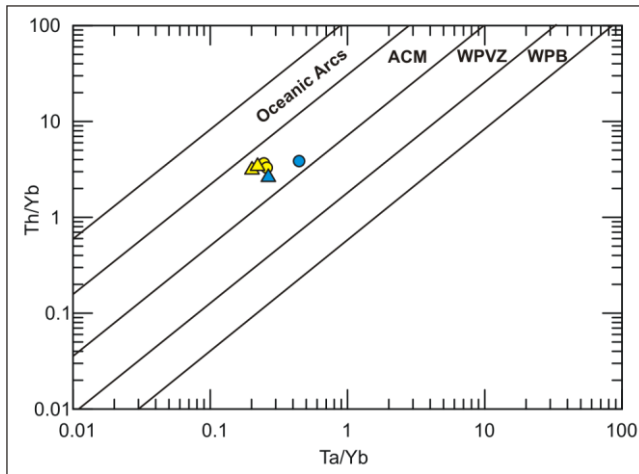


787 Figure 4a: Total alkali vs. silica (TAS) classification diagram (Le Bas et al. 1986) and b:  
788 Zr/TiO<sub>2</sub> vs. Nb/Y classification diagram (Pearce 1996) for the Triassic volcanic rocks of  
789 Transdanubian Range. Data from Kiss (1954), Harangi et al. (1996), Szabó et al. (1996),  
790 Dunkl et al. (2003) and own data. The raw analytical data can be found in the Electronic  
791 Supplementary Material (ESM\_3.xls).



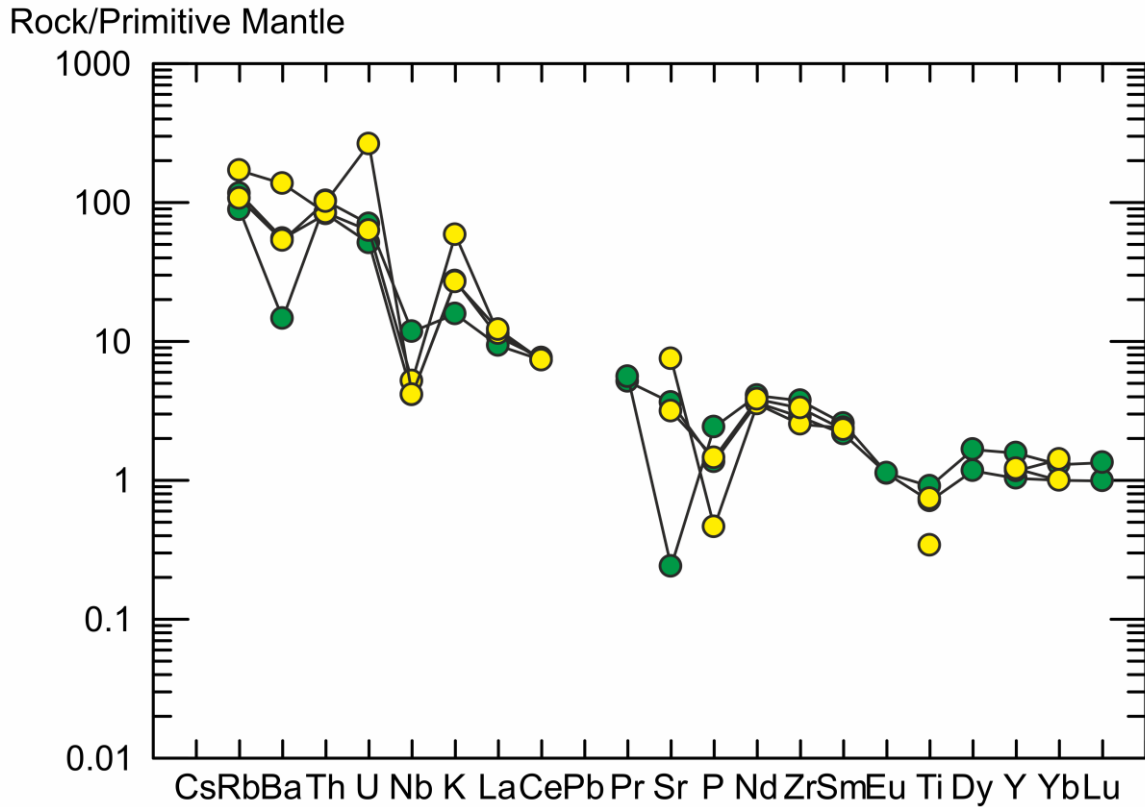
- Bakony Mountains
- Strázsa Hill quarry andesite pebbles
- Strázsa Hill quarry trachyte pebbles
- Strázsa Hill quarry rhyolite pebbles
- Buda Hills andesite dikes and pebbles
- Szár Hill quarry andesite dike

793 Figure 5: Implications for the original tectonomagmatic settings of the Triassic volcanic rocks  
794 of the Transdanubian Range by the discrimination of Gorton and Schandl (2000). Triangles  
795 represent samples with more than 5% LOI. ACM = active continental margins; WPVZ =  
796 within-plate volcanic zones; WPB = within-plate basalts. The legends are the same as in the  
797 Figure 4.



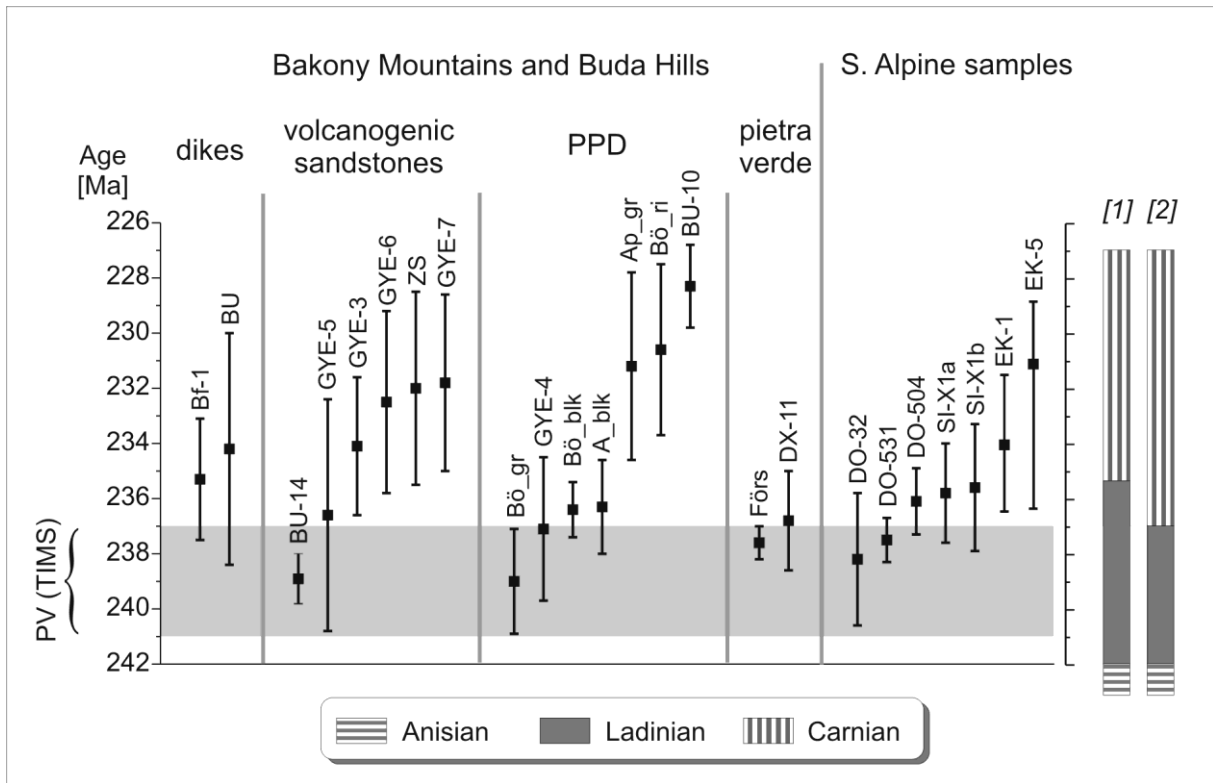
798

799 Figure 6: Multi-element variation diagram for the Triassic volcanic rocks of Transdanubian  
800 Range. Data from Harangi et al. (1996) and own data. The detailed data are in the Electronic  
801 Supplementary Material (ESM\_3.xls). The legends are the same as in the Figure 4.



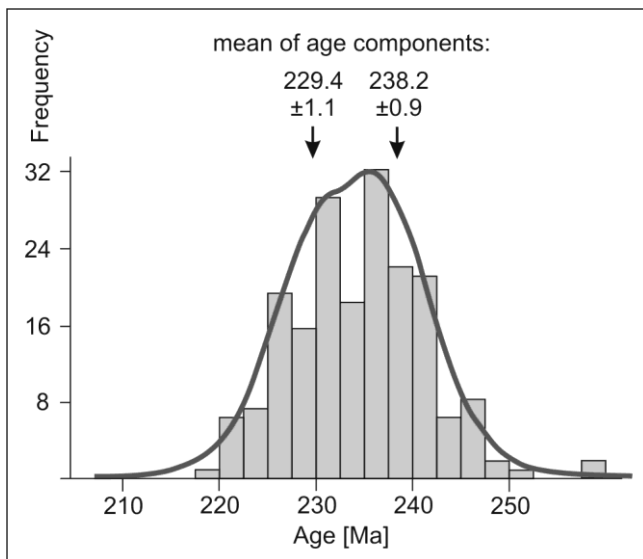
802

803 Figure 7: Compilation of the new LA-ICPMS U-Pb ages obtained on the different Triassic  
 804 volcanic formations of the Transdanubian Range and Southern Alps. PPD: pebble population  
 805 samples compiled from andesite and rhyolite fragments from the Eocene base conglomerate  
 806 covering the denudation surface of the Triassic in the Buda Hills. PV (TIMS): Range of  
 807 'pietra verde' volcanic activity by high resolution U-Pb dating (see text for sources). Right  
 808 panel shows the most recent Triassic time scales; [1]: Mundil et al. (2010), [2]: Cohen et al.  
 809 (2013, updated).



810

811 Figure 8: Compilation of all Triassic zircon U-Pb single-grain ages obtained on the volcanic  
 812 and volcanoclastic formations of the Bakony Mountains and Buda Hills - without the data  
 813 measured on the 'pietra verde' tuff layers. N=274, the Tertiary ages and the inherited, pre-  
 814 Triassic ages are not displayed; bin width=2.5 Myr.

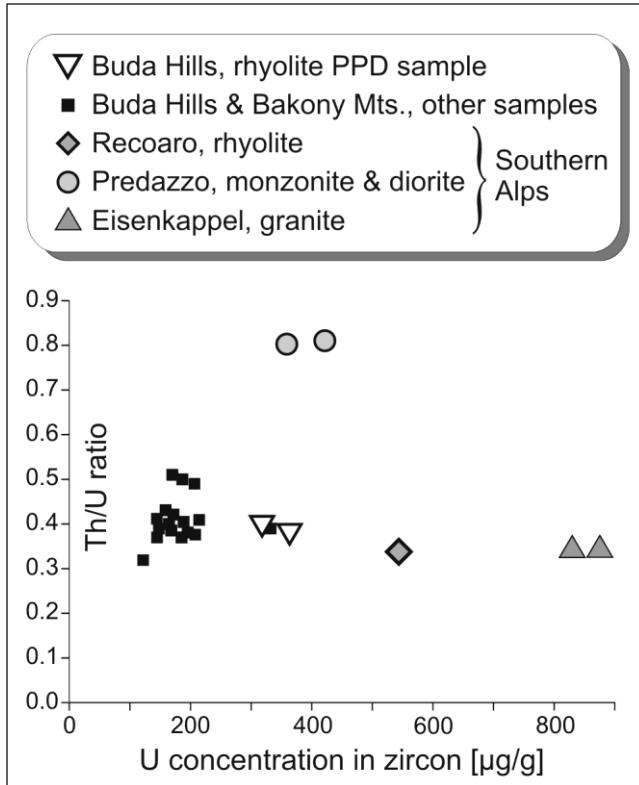


815

816 Figure 9: Actinide composition of the dated zircon samples: median of uranium concentration  
 817 vs. median of Th/U ratio measured in single crystals. Zircons from the Triassic volcanic



818 formations from the Bakony Mountains and Buda Hills form a tight cluster, and it is obvious  
 819 that the samples from the Southern Alps with acid-intermediate composition have different  
 820 actinide element concentrations.



821  
 822 Table 1: Locality and petrography of the samples that yielded usable geochronological results.

823 The entire sample list used for petrographical study is in the Electronic Supplementary  
 824 Material (ESM\_1.xls). PPB indicates pebble population dating according to Dunkl et al.  
 825 (2009).

826  
 827 Table 2: Synopsis of the U–Pb data obtained on the Triassic igneous formations of Bakony  
 828 Mts. and Southern Alps. The raw data can be found in the Electronic Supplementary Material  
 829 (ESM\_6.xls and ESM\_7.pdf).

830  
 831 **Electronic Supplementary Material**

832 Online Resource 1 (ESM\_1.xls): List of samples used for petrographical investigation.

833

834 Online Resource 2: (ESM\_2.pdf): U-Pb ages measured on the zircon reference materials.

835

836 Online Resource 3 (ESM\_3.xls): Whole rock geochemistry of Triassic volcanic formations  
837 from the Transdanubian Range. Oxides and LOI are in wt%, trace elements are in ppm;  
838 missing data: not analysed or below the level of detection.

839

840 Online Resource 4 (ESM\_4.xls): Composition of phenocrysts of the Transdanubian Triassic  
841 volcanic formations determined by electron microprobe analyses.

842

843 Online Resource 5 (ESM\_5.pdf): Composition of phenocrysts of the Transdanubian Triassic  
844 volcanic formations on feldspar (a), pyroxene (b) and amphibole (c) classification diagrams.  
845 The pyroxene and amphibole classifications are based on Morimoto (1988) and on Leake et  
846 al. (1997), respectively. The detailed data can be found in the Electronic Supplementary  
847 Material (ESM\_4.xls).

848

849 Online Resource 6 (ESM\_6.xls): Detailed results of the single-grain U-Pb geochronology.

850

851 Online Resource 7: (ESM\_7.pdf): Age spectra of the individual volcanoclastic samples  
852 plotted by the AgeDisplay software (Sircombe 2004).

Table 1: Locality and petrography of the samples yielded usable geochronological results.  
The entire sample list used for petrographical study is in the Electronic Supplementary Material (ESM\_1.xls).  
PPB indicates pebble population dating according to Dunkl et al. (2009).

Type	Code	Long. [ ° ]	Lat. [ ° ]	Elevation [m]*	Locality / Borehole, depth [m]	Area	Petrography
<b>Andesite dikes</b>							
	BU	18,974	47,471	-577,4	Budaörs-1, 790.4 m	Buda Hills	andesite dike
	Bf-1	19,021	47,409	-1047	Budafok-1, 1147 m	Buda Hills	andesite dike
<b>Volcanogenic sandstones</b>							
	ZS	18,702	47,542	222	Strázsa Hill quarry	Zsámbék basin	volcanoclastite layer
	GYE-5	18,183	47,208	134	Várpalota-3, 37 m	S. Bakony Mts.	volcanoclastite layer
	GYE-6	18,196	47,225	164	Bakonykút-2, 21 m	S. Bakony Mts.	volcanoclastite layer
	GYE-7	"	"	123	Bakonykút-2, 62 m	S. Bakony Mts.	volcanoclastite layer
	GYE-3	18,950	47,463	155	Budaörs, Kálvária Hill	Buda Hills	volcanogenic sandstone
	BU-14	18,952	47,462	150	Budaörs, Kálvária Hill	Buda Hills	volcanogenic sandstone
<b>Pebble-population samples from the base of the Eocene transgressive sequence</b>							
	Bö_blk	18,955	47,464	193	Budaörs, Kő Hill	Buda Hills	black andesite PPD-1
	A_blk	"	"	"	"	"	black andesite PPD-2
	Bö_gr	"	"	"	"	"	green acid volcanic PPD-1
	AP_gr	"	"	"	"	"	green acid volcanic PPD-2
	Bö_ri	"	"	"	"	"	rhyolite tuff PPD
	BU-10	18,931	47,523	332	Budakeszi sanatorium	Buda Hills	andesite PPD
	GYE-4	19,036	47,590	225	Róka Hill	Buda Hills	andesite PPD
<b>Pietra verde</b>							
	Förs	17,943	47,018	230	Felsőörs	S. Bakony Mts.	bentonitic trachite tuff
	DX-11	18,020	47,134	195	Hajmáskér	S. Bakony Mts.	bentonitic trachite tuff
<b>Triassic igneous samples from the eastern Southern Alps</b>							
	DO-531	11,589	46,314	1310	Predazzo W	Dolomites	monzonite
	DO-504	11,603	46,307	1052	Predazzo-Bellamonte	Dolomites	mela-diorite
	DO-32	11,221	45,721	660	Recoaro N	S. Alps	rhyolite
	SI-X1a	13,653	46,596	1110	Nötsch im Gailtal	Drauzug	tuffite
	EK-1	14,590	46,477	610	Eisenkappel	Drauzug	granite
	EK-5	14,614	46,475	733	Eisenkappel	Drauzug	granite

\*: at boreholes the true elevation of the sample relatively to sea level is indicated

Table 2: Synopsis of the U–Pb data obtained on the Triassic igneous formations of Bakony Mts. and Southern Alps. The raw data can be found in the Electronic Supplementary Material (ESM\_6.xls and ESM\_7.pdf).

Type	Sample	Locality & lithology	No. of data	U* [ppm]	Th/U* ratio	Concordia Age [Ma]	± **	TuffZirc Age [Ma]	+	-
<b>Andesite dikes</b>										
	BU	Budaörs-1 borehole, 790.4 m, andesite dike	18	147	0,39			<b>234,2</b>	4,2	2,9
	Bf-1	Budafok-1 borehole, 1147 m, andesite dike	18	162	0,40	<b>235,3</b>	2,2			
<b>Volcanogenic sandstones</b>										
	ZS	Strázsa Hill quarry, volcanoclastite layer	20	332	0,39			<b>232,0</b>	3,5	1,4
	GYE-5	Várpalota-3 borehole, 37 m, volcanoclastite	6	186	0,50	<b>236,6</b>	4,2			
	GYE-6	Bakonykút-2 borehole, 21 m, volcanoclastite	11	144	0,41	<b>232,5</b>	3,3			
	GYE-7	Bakonykút-2 borehole, 62 m, volcanoclastite	9	158	0,43	<b>231,8</b>	3,2			
	GYE-3	Budaörs, Kálvária Hill, volcanoclastic sandstone	19	185	0,37	<b>234,1</b>	2,5			
	BU-14	Budaörs, Kálvária Hill, volcanoclastic sandstone	88	207	0,38			<b>238,9</b>	0,9	0,9
<b>Pebble-population samples from the base of the Eocene transgressive sequence</b>										
	A_blk	Budaörs, Kő Hill, black andesite PPD-2	18	168	0,42	<b>236,3</b>	1,7			
	Bö_blk	Budaörs, Kő Hill, black andesite PPD-1	9	145	0,37	<b>236,4</b>	1,0			
	AP_gr	Budaörs, Kő Hill, green acid volcanic tuff PPD-2	26	165	0,40			<b>231,2</b>	3,4	2,9
	Bö_gr	Budaörs, Kő Hill, green acid volcanic tuff PPD-1	26	317	0,40			<b>239,0</b>	1,9	2,4
	Bö_ri	Budaörs, Kő Hill, rhyolite tuff PPD	23	363	0,38	<b>230,6</b>	3,1			
	BU-10	Budakeszi sanatorium, andesite PPD	20	195	0,38	<b>228,3</b>	1,5			
	GYE-4	Róka Hill andesite PPD	8	186	0,40			<b>237,1</b>	2,6	2,6
<b>Pietra verde samples from the Bakony Mountains</b>										
	Förs	Felsőörs, pietra verde tuff	20	121	0,32			<b>237,6</b>	0,6	1,6
	DX-11	Hajmáskér, pietra verde tuff	20	170	0,51			<b>236,8</b>	1,8	2,7
<b>Triassic igneous samples from the eastern Southern Alps</b>										
	DO-531	Predazzo W, monzonite	22	421	0,81	<b>237,5</b>	0,8			

DO-504	Predazzo E, mela-diorite	18	357	0,80			<b>236,1</b>	1,2	1,3
DO-32	Recoaro, rhyolite	23	543	0,34			<b>238,2</b>	2,4	2,5
SI-X1a	Nötsch, tuffite	26	214	0,41			<b>235,8</b>	1,8	2,1
SI-X1b	Nötsch, tuffite	16	206	0,49			<b>235,6</b>	2,3	1,7
EK-1	Eisenkappel, granite	12	877	0,34	<b>234,1</b>	2,5			
EK-5	Eisenkappel, granite	14	825	0,34			<b>231,2</b>	5,8	2,2

The U concentration and the Th/U ratio are calculated as median.

\*: calculated only for the crystals yielding Triassic U-Pb age

\*\* : uncertainty of concordia ages as 95% confidence